

KIC 10975348: A double-mode or triple-mode high-amplitude δ Scuti star?

Tao-Zhi Yang¹, Xiao-Ya Sun¹, Zhao-Yu Zuo^{1,*}, Hai-Wen Liu²

ABSTRACT

In this paper, we analyze the light variations of KIC 10975348 using photometric data delivered from *Kepler* mission. This star is exceptionally faint ($K_p = 18.6$ mag), compared to most well-studied δ Scuti stars. The Fourier analysis of the short cadence data (i.e. Q14, Q15 and Q16, spanning 220 days) reveals the variations are dominated by the strongest mode with frequency $F_0 = 10.231899 \text{ d}^{-1}$, which is compatible with that obtained from *RATS-Kepler*. The other two independent modes with $F_1 (= 13.4988 \text{ d}^{-1})$ and $F_2 (= 19.0002 \text{ d}^{-1})$ are newly detected and have amplitudes two orders of magnitude smaller than F_0 . We note that, for the first time, this star is identified to be a high-amplitude δ Sct (HADS) star with amplitude of about 0.7 mag, and the lower ratio of $F_0/F_1 = 0.758$ suggests it might be a metal-rich variable star. The frequency F_2 may be a third overtone mode, suggesting this target might be a new radial triple-mode HADS star. We perform $O-C$ analysis using 1018 newly determined times of maximum light and derive an ephemeris formula: $T_{\max} = 2456170.241912(0)+0.097734(1) \times E$. The $O-C$ diagram shows that the pulsation period of KIC 10975348 seems to show no obvious change, which is in contrast to that of the majority of HADS stars. The possible cause of that may be due to the current short time span of observations. To verify its possible period variations, regular observation from space with a longer time span in future is needed.

Subject headings: stars: oscillations; stars: variable: delta Scuti

1. Introduction

The main scientific goal of the *Kepler Mission* was to search for Earth-like planets outside the solar system by detecting transits of the host star (Koch et al. 2010; Borucki et al. 2010). The high-precision photometric data delivered from *Kepler* telescope also provides an unprecedented opportunity to probe into stellar interiors using their natural oscillation modes, and hence greatly

¹ School of Physics, Xi'an Jiaotong University, 710049 Xi'an, PR China; e-mail: zuozyu@xjtu.edu.cn;

² School of Information and Communications Engineering, Xi'an Jiaotong University, 710049 Xi'an, PR China;

expands the field of asteroseismology (Chaplin et al. 2010). Thanks to the ultra-high precision photometric observations at the level of μmag , our understanding of many types of pulsating stars has been significantly improved. For instance, Bedding et al. (2011) reported that in red giants the hydrogen- and helium-burning stars can be distinguished according to the observed period spacings of gravity modes; Giambicheli et al. (2018) found a pulsating white dwarf has a large oxygen-dominated core, which exceeds the predictions of existing models of stellar evolution. As a common group of variable stars, δ Scuti stars are excellent target for asteroseismic study. At present, more than 2000 δ Scuti stars have been found in the *Kepler* field (Balona & Dziembowski 2011; Balona 2014; Bowman et al. 2016), however, only several high-amplitude δ Scuti stars are found and investigated in detail so far (Balona et al. 2012; Yang et al. 2018b; Yang & Esamdin 2019).

High-amplitude δ Sct (HADS) stars, as a subgroup of δ Sct stars, are usually recognized by their relatively simple, non-sinusoidal light variations with peak-to-peak amplitude larger than 0.3 mag (Breger 2000). They are slow rotators with $v \sin i < 30 \text{ km s}^{-1}$ and the slow rotation might be a precondition for their high amplitudes (Breger 2000). In the H-R diagram, HADS stars seem to concentrate in a narrow strip in the δ Sct instability region with a width of about 300 K in temperature (McNamara 2000), but observations from space photometry revealed that some HADS stars can also be found beyond the narrow region (Balona 2016). The light variations of HADS stars are usually dominated by the fundamental and/or first overtone radial mode(s) (Breger 2000; McNamara 2000). Although the AAVSO International Variable Star Index (VSX) (Watson et al. 2015) lists almost 600 HADS stars, radial triple-mode HADS stars are particular rare. Only five HADS stars with three consecutive radial modes, i.e. AC And (Fitch & Szeidl 1976), V823 Cas (Jurcsik et al. 2006), V829 Aql (Handler et al. 1998), GSC 762-110 (Wils et al. 2008) and GSC 03144-595 (Mow et al. 2016), are found at present.

In recent decades, nonradial modes with low amplitude are also detected in some HADS stars, owing to extensive high-precision photometric observations (Poretti et al. 2011). Moreover, with the advent of space asteroseismology, long-term variations of the principal modes and more low-amplitude frequencies are detected in HADS stars. Balona et al. (2012) reported a slight amplitude variation of the dominant modes in the HADS star V2367 Cyg and also found this star rotates with a twice the projected rotational velocity of any other HADS star. With *Kepler* observations, amplitude modulation in several HADS stars was investigated. Yang et al. (2018b) found a pair of low-amplitude triplet structures in the frequency spectra of KIC 5950759 and the reason for this triplet structure might be the amplitude modulation of stellar rotation. Another HADS star KIC 10284901 also shows a weak amplitude modulation with two frequencies, and analysis suggests that they might be related to the Blazhko effect (Yang & Esamdin 2019). Hence, the identification of these low-amplitude frequencies in HADS stars possesses great potential to improve our understanding of the stellar interior, and the comparison of single-, double- and triple-

mode HADS stars may illuminate what determines the number of radial modes in which a star pulsates. More HADS stars with high-precision photometric observations are needed.

KIC 10975348 ($\alpha_{2000}=19^h26^m46^s.1$, $\delta_{2000}=+48^\circ25'30''$.8, 2MASS: J1926461+4825303) was classified as a δ Sct star with a pulsation period of 2.35 hrs by Ramsay et al. (2014). In that paper, KIC 10975348 was reported as a mid A type star based on spectrum from Gran Telescopio Canarias (GTC). Some basic parameters of this target were listed in Table 1. According to the amplitude of the light curves, KIC 10975348 appears to be a HADS star, yet the exact type is uncertain. In this work, using the high-precision photometric data from *Kepler* mission, we further verify its nature, and investigate its long-term periodic variation as well.

2. OBSERVATIONS AND DATA REDUCTION

KIC 10975348 was observed by *Kepler* space telescope from BJD 2456107.139 to 2456424.001, including three quarters (i.e. Q14, Q15 and Q16). There are two observation strategies for this star: Long cadence (LC: 29.5-min integration time) mode and Short cadence (SC: 58.5-s integration time). To avoid the Nyquist alias peaks, we only used the SC data, i.e. Q14.3, Q15.3 and Q16.3 in this work. More details on how to identify the Nyquist alias peaks in LC data can be found in Murphy et al. (2013) and Yang et al. (2018b). All the SC data are available in Kepler Asteroseismic Science Operations Center (KASOC) data base¹(Kjeldsen et al. 2010), in which two types of data: "raw" flux and "corrected" flux, are provided. The former data has been reduced by the NASA *Kepler* Science pipeline in fact, and the "corrected" one can be obtained from KASOC Working Group 4 (WG#4: δ Sct stars). The corrected flux was used in this work and we first performed several corrections to the data including removing the obvious outliers and de-trending the light curve with a low-order polynomial. Then the flux data was converted to the magnitude scale, and each quarter was adjusted to zero by subtracting their mean value. The final rectified light curve was obtained with 147481 data points in total, spanning over about 220 days. Figure 1 shows a portion of the rectified light curve of KIC 10975348 covering 2 days. From this figure, it is clear that the amplitude of the light curve is about 0.7 mag, which is larger than the typical amplitude (> 0.3 mag) of high-amplitude δ Sct star.

¹KASOC data base: <http://kasoc.phys.au.dk>

Table 1. Basic Properties of KIC 10975348

Parameters	KIC 10975348	References
K_P	18.598 mag	a
P	2.35 h	b
i	18.496 mag	a
g	18.89 mag	b
$U-g$	0.19 mag	b
$g-r$	0.34 mag	b

Note. — (a) These parameters are available in the KASOC: <https://kasoc.phys.au.dk/>; (b) Ramsay et al. 2014.

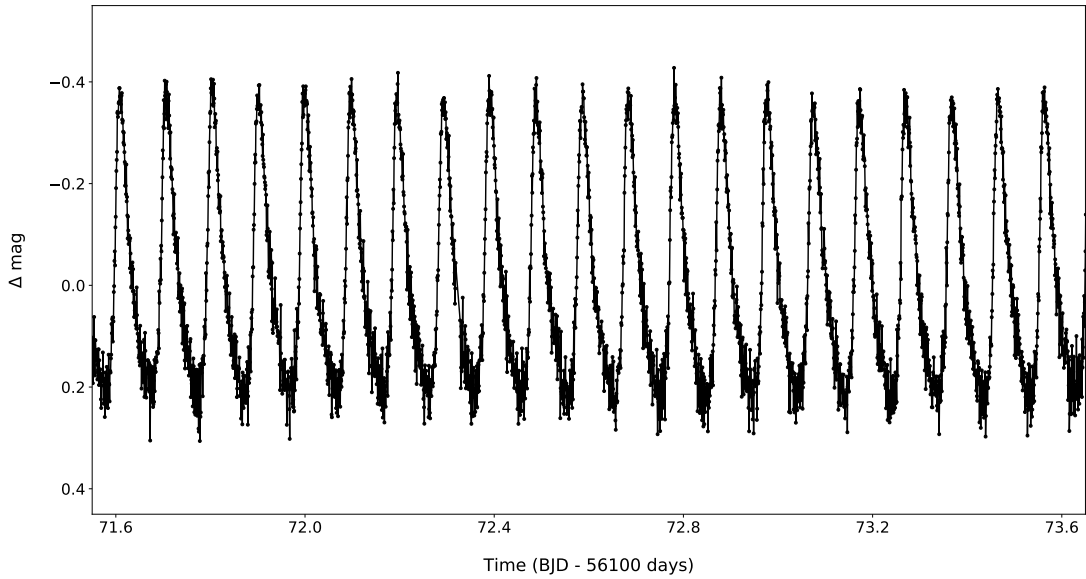


Fig. 1.— A portion of the short cadence light curve of KIC 10975438. The amplitude of the light curve is about 0.7 mag, revealing that it may be a HADS star.

3. FREQUENCY ANALYSIS

We used the software PERIOD04 (Lenz & Breger 2005) to analyze the pulsating behavior of KIC 10975348. The rectified light curve was fitted with the following formula:

$$m = m_0 + \sum A_i \sin(2\pi(f_i t + \phi_i)), \quad (1)$$

where m_0 , A_i , f_i , and ϕ_i are zero-point, amplitude, frequency and the corresponding phase, respectively.

In order to detect more significant frequencies, we chose a frequency range of $0 < \nu < 80$ d⁻¹, which is wider than the typical period range of δ Scuti stars. During the extraction of significant frequency, the highest peak was usually selected as a potential significant frequency. Then a multi-frequency least-square fit using formula 1 was applied to the light curve with all significant frequencies detected, and obtained the solutions for all the frequencies. A theoretical light curve constructed by the above solutions was subtracted from the rectified data and the residual was obtained for next search. The above steps were repeated until there was no significant peak in the frequency spectrum. The criterion of S/N > 4.0 suggested by Breger et al. (1993) was adopted to judge the significance of the detected peaks. The uncertainties of frequencies were obtained following the method provided by Montgomery & O'donoghue (1999).

Figure 2 shows the amplitude spectra and the prewhitening procedures of the light curve. The last panel shows amplitude spectra after 11 detected frequencies were pre-whitened. Following Breger et al. (1993), we draw the significance curves at signal-to-noise ratio S/N = 4 in last panel for the judgement of a significant peak. There is no significant peak in the residuals and the overall distribution of the residual is typical of noise.

A total of 11 significant frequencies were detected in this work and a full list was given in Table 2. Among these frequencies, three stronger frequencies were considered to be independent. It is reasonable that the strongest peak f_{S1} was assumed to be the fundamental mode, since the light variations were dominated by this frequency. Therefore, we marked f_{S1} with 'F0' in the last column of Table 2. In addition, six harmonics of F0 were also detected and listed in the table. The other two independent frequencies are f_{S8} and f_{S10} , we marked them with 'F1' and 'F2', respectively. The rest of the frequencies are combinations with F0.

For frequencies F0 and F1, we found the period ratio of $P_1/P_0 = F0 / F1 = 0.758$ was in the typical range (0.756 - 0.787) of period ratio of the first overtone and fundamental mode for δ Scuti stars (Petersen & Christensen-Dalsgaard 1996). It seems that F1 can be identified as the first overtone mode. Considering its peak-to-peak amplitude over 0.7 mag from the light curve, KIC 10975348 seems to be classified as a new double-mode HADS star.

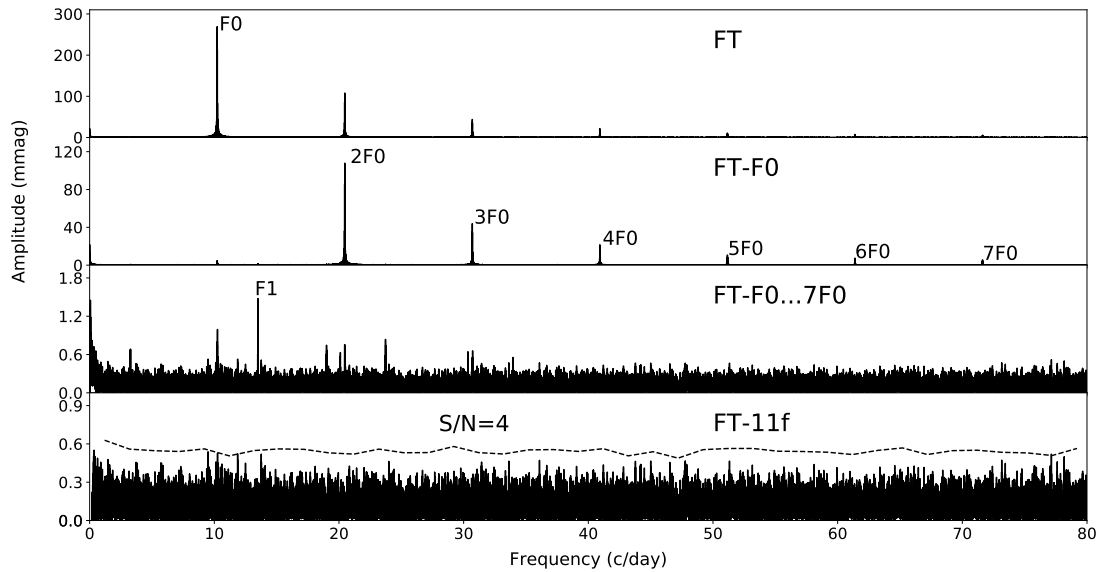


Fig. 2.— Fourier amplitude spectra and the pre-whitening process for the light curve of KIC 10975348. The first two panels show F0 and its 6 harmonic frequencies. The third panel is the amplitude spectra after subtracting F0 and its harmonic frequencies, where the independent frequency F1 is marked. The bottom panel shows the residual after subtracting 11 significant frequencies. The dotted curve refers to detection limit of $S/N = 4.0$.

4. $O-C$ Diagram

To examine the potential long-term period changes of KIC 10975348, a classical $O-C$ diagram was constructed. O is the observed time of maximum light and C is the theoretical value from ephemeris formula (Sterken 2005). For the calculations of O , we first visually inspected the light curve and determined the preliminary times of maximum, and then made a second-order polynomial to fit the part of light curve around one-third of the full amplitude. It is reasonable to do that since this part of light curve is almost symmetric for this star. The times of extremum of the polynomial fit were considered as the observed times of maximum light. The typical uncertainties (about 0.00008 d^{-1}) were estimated by Monte Carlo simulations. In total, 1018 times of maximum light were obtained and a full list of each quarter is given in Table 3, 4 and 5, respectively.

To obtain the calculated times of maximum light, we used all the observed times of maximum and derived a new ephemeris formula:

$$T_{max} = T_0 + P \times E = 2456170.241912(0) + 0.097734(1) \times E. \quad (2)$$

where T_0 is the initial epoch, P is the period, and E is the cycle number.

Then the values of $O-C$ were derived based on this new ephemeris. All the $O-C$ values, as well as the corresponding cycle numbers are listed in Table 3, 4 and 5, respectively.

Figure 3 shows the $O-C$ diagram of three quarters used in this work. It is noteworthy that the $O-C$ of each quarter is almost flat, which suggests the star seems to have no obvious period change.

5. DISCUSSION

5.1. Double-mode or multi-mode?

HADS stars are usually single- or double-mode radial pulsators (Breger 2000). As mentioned above, in KIC 10975348, the first two stronger frequencies F0 and F1 give a period ratio of $P1/P0 = 0.758$, suggesting this star appears to be a double-mode HADS star. A detailed diagram about the double-mode HADS stars and metallicities were given by Petersen & Christensen-Dalsgaard (1996). Their study showed that higher values of the period ratio can be found in metal-poor stars. For KIC 10975348, the lower period ratio of 0.758 implies it might be a metal-rich double-mode HADS star.

The third independent frequency F2 ($=19.0002 \text{ d}^{-1}$) is interesting. Identification of this fre-

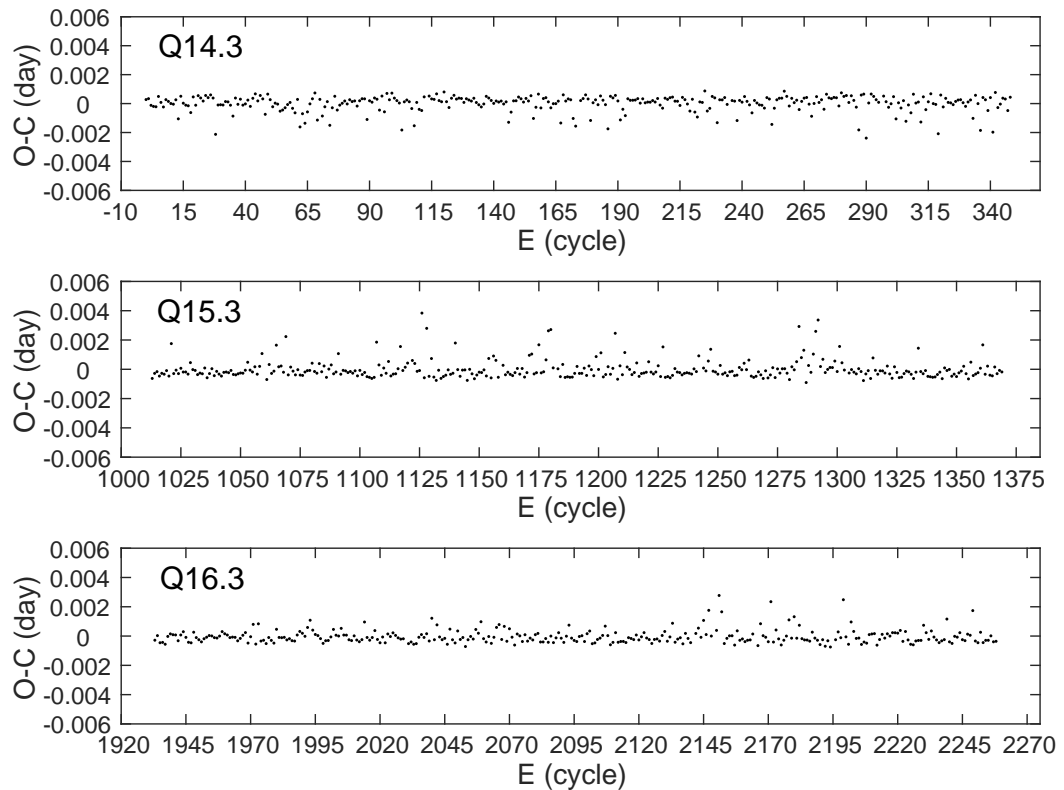


Fig. 3.— $O-C$ diagram of KIC 10975348, based on a collection of 1018 times of maximum light. Upper panel: The $O-C$ of Q14.3 changes over time. Middle panel: The $O-C$ of Q15.3 changes over time. Lower panel: The $O-C$ of Q16.3 changes over time. None of these panels shows a significant trend, indicating that the pulsation period has no significant change.

quency is very important, as the pulsating stars with three radial modes are very rare at present (Wils et al. 2008; Mow et al. 2016). Stellingwerf (1979) calculated a series of stellar modes for δ Scuti stars and presented the period ratios of the first four radial modes as: $P_1/P_0 = (0.756 - 787)$, $P_2/P_0 = (0.611 - 632)$ and $P_3/P_0 = (0.500 - 525)$, in which P_0 , P_1 , P_2 and P_3 present the fundamental mode, first overtone, second overtone and third overtone, respectively. For KIC 10975348, the ratio of F0/F2 (= 0.539) is between P_2/P_0 and P_3/P_0 , but close to P_3/P_0 . It seems to indicate F2 might be a third radial overtone. To determine the exact nature of F2, detailed seismic modelling and multi-color photometric observations are still required. We note such models about the period ratios are still lacking (Lovekin & Guzik 2017; Daszyńska-Daszkiewicz et al. 2020; Rodríguez-Martín et al. 2020). We suggest more studies of models (linear or nonlinear) investigating expected period ratios and effects on input physics for HADS stars should be undertaken. If confirmed, KIC 10975348 would be a new radial triple-mode HADS star, and hence enrich the sample of triple-mode variables.

From ground-based observations, some HADS stars are the so-called mono-period pulsating variables, e.g. YZ Boo (Yang et al. 2018), XX Cyg (Yang et al. 2012), etc. They usually pulsate with a fast rising from minimum to maximum light and a slow declining, and their light amplitudes are nearly constant. The light curve of KIC 10975348 is similar to that of these stars, but it was identified as a double-mode HADS star, since a low-amplitude first overtone was detected in this star owing to the high-precision photometric observations from space. For instance, in the Fourier amplitude spectra of YZ Boo, the typical amplitudes of noise of the residual are 1.5 mmag, while in KIC 10975348, the second independent frequency F1 has an amplitude of only 1.5 mmag, so that such a weak amplitude will certainly fall in the noise if the observations are obtained from the ground and with relatively short time-series observations. This naturally raises such questions: Will the current so-called mono-period HADS stars become double- or multi- mode stars in the space era? Is there any real mono-period HADS star? What about the relation between the mono- and double-mode HADS stars and their stellar parameters? These questions are of importance for the study of HADS stars, particularly for their seismic modellings. The all-sky *TESS* observations of HADS stars could provide a well-timed opportunity to address these questions and improve our knowledge of HADS stars.

5.2. $O-C$

The period changes due to stellar evolution for stars in and across the lower part of the classical instability strip allow an observational test of stellar evolution theory, assuming that other physical reasons for period changes can be excluded (Breger 2000). From a theoretical point of view, an

evolutionary change in T_{eff} and M_{bol} leads to a period change of size (equation 9 of Breger 2000)

$$\frac{1}{P} \frac{dP}{dt} = -0.69 \frac{dM_{bol}}{dt} - \frac{3}{T_{eff}} \frac{dT_{eff}}{dt} + \frac{1}{Q} \frac{dQ}{dt} \quad (3)$$

where P is the period of a radial pulsation mode in unit of days, Q is the pulsation constant. For a specific mode, the Q value is essential constant for all δ Scuti stars, hence the term $(1/Q)/(dQ/dt)$ is negligible as it is a very small quantity (Breger 2000). The above relation is then reduced to as follows,

$$\frac{1}{P} \frac{dP}{dt} = -0.69 \frac{dM_{bol}}{dt} - \frac{3}{T_{eff}} \frac{dT_{eff}}{dt} \quad (4)$$

In the lower instability strip where the δ Scuti stars are found, stellar evolution leads to increasing periods in most of stars, with predicted increase period changes from 10^{-10} yr $^{-1}$ for the stars on the main sequence to 10^{-7} yr $^{-1}$ for the longer-period evolved variable stars (Breger & Pamyatnykh 1998). Such period changes are observable and also have been observed in some radial δ Scuti pulsators. Breger & Pamyatnykh (1998) calculated the theoretical periods of the radial fundamental modes and their changes during late main-sequence and post-main-sequence evolution of the $1.8 M_\odot$ model and found the observations are consistent with the predicted values. Xue et al. (2018) investigated a HADS star VX Hya with the observed period change from $O-C$ and the stellar evolutionary models, and found the period change can be successfully interpreted by the evolutionary effect.

In pulsating stars, when a pulsation period changes linearly with time, the $O-C$ diagram will present a parabolic form that rises or falls depending on whether the period is increasing or decreasing (Sterken 2005). For HADS stars, the $O-C$ diagram is a powerful tool to investigate their period changes. According to Breger (2000), HADS stars can be divided into two groups depending on whether the period change is increasing or decreasing. For instance, some HADS stars have an increasing period, i.e., YZ Boo (Yang et al. 2018); XX Cyg (Yang et al. 2012); GP And (Zhou & Jiang 2011), etc., while others pulsate with a decreasing period, such as: BS Aqr (Boonyarak et al. 2011); BE Lyn (Boonyarak et al. 2011); DY Peg (Blake et al. 2003), etc. Different values of period changes may suggest stars are in different stages of evolution.

For KIC 10975348 in this work, it was also expected to exhibit an increasing or decreasing period. However, from $O-C$ diagram in Figure 3, it seems that the shape of $O-C$ is nearly flat and does not show any curved part, which is in contrast to the predictions by Breger (2000). The possible cause for that might be due to the shorter time span of the observations for this star. To verify its period variations, theoretical seismic modelling and regular observations from space with a longer time span in the future are necessary.

6. SUMMARY

We analyzed the pulsating behavior of KIC 10975348 using high-precision photometric observations from *Kepler* mission, and detected 11 significant frequencies from SC data. Among these frequencies, three independent frequencies, i.e. $F_0 = 10.231899 \text{ d}^{-1}$, $F_1 = 13.4988 \text{ d}^{-1}$ and $F_2 = 19.0002 \text{ d}^{-1}$ were found. The lower period ratio ($=0.758$) of the first two stronger frequencies (i.e. F_0 and F_1) suggests that KIC 10975348 might be a metal-rich double-mode HADS star. The third independent frequency might be a third overtone mode. If confirmed, KIC 10975348 would be a new radial triple-mode HADS star, and hence enrich the rare sample of pulsating stars with three radial modes. We also compared KIC 10975348 with current mono-period HADS stars, and highlighted the potential of *TESS* mission for the study of HADS stars.

The $O-C$ diagram was constructed with 1018 times of maximum light and yielded a new ephemeris epoch: $T_{max}=T_0+P\times E=2456170.241912(0)+0.097734(1)\times E$. The $O-C$ analysis indicated that the period of KIC 10975348 shows no obvious change, which is very unusual. The cause of that might be due to the shorter time span of current observations. To verify the evolutionary state of KIC 10975348, regular observations from space in the future are necessary.

We thank the referee for his/her comments that help clarify the paper. This research is supported by the National Natural Science Foundation of China (grant Nos. 11573021, U1938104, 12003020) and the Fundamental Research Funds for the Central Universities. We would like to thank the *Kepler* science team for providing such excellent data.

REFERENCES

- Balona L. A., Dziembowski W. A., 2011, MNRAS, 417, 591-601
Balona L. A., Lenz P., Antoci V., et al., 2012, MNRAS, 419, 3028-3038
Balona L. A., 2014, MNRAS, 437, 1476-1484
Balona, L. A. 2016, MNRAS, 459, 1097
Bedding T. R., Mosser B., Huber D., et al., 2011, Nature, 471, 608
Blake, R. M., Delaney, P., Khosravani, H., et al. 2003, PASP, 115, 212
Boonyarak, C., Fu, J.-N., Khokhundod, P., et al. 2011, Ap&SS, 333, 125
Borucki W. J., Koch D., Basri G., et al., 2010, Science, 327, 977

- Bowman D. M., Kurtz D. W., Breger M., et al., 2016, MNRAS, 460, 1970-1989
- Breger, M., Stich, J., Garrido, R., et al. 1993, A&A, 271, 482
- Breger, M. & Pamyatnykh, A. A. 1998, A&A, 332, 958
- Breger, M. 2000, Delta Scuti and Related Stars, 210, 3
- Chaplin, W. J., Appourchaux, T., Elsworth, Y., et al. 2010, ApJ, 713, L169
- Daszyńska-Daszkiewicz, J., Pamyatnykh, A. A., Walczak, P., et al. 2020, MNRAS, 499, 3034.
doi:10.1093/mnras/staa3056
- Fitch, W. S. & Szeidl, B. 1976, ApJ, 203, 616. doi:10.1086/154120
- Giammichele N., Charpinet S., Fontaine G., et al. 2018, Nature, 554, 73
- Kjeldsen H., Christensen-Dalsgaard J., Handberg R., et al., 2010, Astronomische Nachrichten, 331, 966
- Jurcsik, J., Szeidl, B., Váradi, M., et al. 2006, A&A, 445, 617. doi:10.1051/0004-6361:20052876
- Handler, G., Pikall, H., & Diethelm, R. 1998, Information Bulletin on Variable Stars, 4549, 1
- Koch, D. G., Borucki, W. J., Basri, G., et al. 2010, ApJ, 713, L79
- Lenz P., Breger M. 2005, CoAst, 146, 53
- Lovekin, C. C. & Guzik, J. A. 2017, ApJ, 849, 38. doi:10.3847/1538-4357/aa8e01
- McNamara D. H., 2000, in Delta Scuti and Related Stars., M. Breger, & M. H. Montgomery, ASP Conf.Ser., 210, 373
- Mow, B., Reinhart, E., Nhim, S., et al. 2016, AJ, 152, 17
- Murphy, S. J., Shibahashi, H., & Kurtz, D. W. 2013, MNRAS, 430, 2986.
doi:10.1093/mnras/stt105
- Montgomery M. H., & O'donoghue D., 1999, Delta Scuti Star Newsletter, 13, 28
- Petersen, J. O. & Christensen-Dalsgaard, J. 1996, A&A, 312, 463
- Poretti, E., Rainer, M., Weiss, W. W., et al. 2011, A&A, 528, A147
- Ramsay G., Brooks A., Hakala P., et al., 2014, MNRAS, 437, 132

Rodríguez-Martín, J. E., García Hernández, A., Suárez, J. C., et al. 2020, MNRAS, 498, 1700.
doi:10.1093/mnras/staa2378

Stellingwerf, R. F. 1979, ApJ, 227, 935

Sterken, C. 2005, The Light-Time Effect in Astrophysics: Causes and cures of the O-C diagram,
335, 3

Watson, C., Henden, A.I., Price, A. 2015, International Variable Star Index VSX (Cambridge, MA:
AAVSO), <https://www.aavso.org.vsx>

Wils, P., Rozakis, I., Kleidis, S., et al. 2008, A&A, 478, 865

Xue, H.-F., Fu, J.-N., Fox-Machado, L., et al. 2018, ApJ, 861, 96. doi:10.3847/1538-4357/aac9c5

Yang, X. H., Fu, J. N., & Zha, Q. 2012, AJ, 144, 92

Yang, T.-Z., Esamdin, A., Fu, J.-N., et al. 2018, Research in Astronomy and Astrophysics, 18, 002

Yang, T., Esamdin, A., Song, F., et al. 2018, ApJ, 863, 195

Yang, T.-Z. & Esamdin, A. 2019, ApJ, 879, 59

Zhou, A.-Y. & Jiang, S.-Y. 2011, AJ, 142, 100

Table 2. A full list of 11 significant frequencies detected in this work (denoted by f_{Si}).

f_{Si}	Frequency (d^{-1})	Amplitude (mmag)	S/N	Identification
1	10.231899(1)	269.1	984.6	F0
2	20.463798(3)	107.9	634.7	2F0
3	30.695470(7)	43.9	270.8	3F0
4	40.92731(2)	21.5	151.4	4F0
5	51.15921(3)	10.8	75.7	5F0
6	61.39110(4)	7.5	57.0	6F0
7	71.62278(6)	5.6	39.6	7F0
8	13.4988(2)	1.5	9.6	F1
9	23.7314(4)	0.8	5.8	F0+F1
10	19.0002(5)	0.7	5.4	F2
11	33.9629(6)	0.5	4.1	2F0+F1

Note. — Among these frequencies, 3 peaks are independent frequencies, others are harmonic or combinations.

Table 3. 345 times of Maximum Light and $O-C$ Values of Q14.3.

BJD (2400000+)	E	$O-C$ (day)	BJD (2400000+)	E	$O-C$ (day)	BJD (2400000+)	E	$O-C$ (day)
56170.242260	0	0.000278	56181.579400	116	0.000291	56192.916480	232	0.000256
56170.340060	1	0.000340	56181.677510	117	0.000671	56193.014380	233	0.000416
56170.437330	2	-0.000121	56181.774780	118	0.000206	56193.111640	234	-0.000058
56170.534990	3	-0.000196	56181.872430	119	0.000127	56193.307370	236	0.000210
56170.632700	4	-0.000220	56181.970840	120	0.000802	56193.405070	237	0.000169
56170.731140	5	0.000492	56182.067900	121	0.000131	56193.501460	238	-0.001173
56170.828470	6	0.000082	56182.165230	122	-0.000273	56193.600580	239	0.000219
56170.925880	7	-0.000235	56182.263610	123	0.000369	56193.698200	240	0.000099
56171.024120	8	0.000271	56182.361550	124	0.000571	56193.796320	241	0.000486
56171.121740	9	0.000150	56182.459020	125	0.000309	56193.893720	242	0.000153
56171.219320	10	0.000004	56182.556820	126	0.000377	56193.991210	243	-0.000090
56171.317010	11	-0.000042	56182.654530	127	0.000352	56194.088390	244	-0.000641
56171.415050	12	0.000262	56182.751990	128	0.000081	56194.186980	245	0.000216
56171.511470	13	-0.001055	56182.849980	129	0.000335	56194.284540	246	0.000041
56171.610760	14	0.000507	56182.947630	130	0.000248	56194.382140	247	-0.000091
56171.708020	15	0.000026	56183.045290	131	0.000173	56194.479850	248	-0.000116
56171.805610	16	-0.000110	56183.143220	132	0.000370	56194.577390	249	-0.000312
56171.903310	17	-0.000151	56183.240650	133	0.000075	56194.675850	250	0.000412
56172.000570	18	-0.000622	56183.338230	134	-0.000082	56194.773480	251	0.000314
56172.099380	19	0.000460	56183.435810	135	-0.000233	56194.869460	252	-0.001440
56172.196550	20	-0.000113	56183.533750	136	-0.000029	56194.968320	253	-0.000321
56172.294940	21	0.000547	56183.632020	137	0.000501	56195.066630	254	0.000261
56172.392510	22	0.000388	56183.729630	138	0.000384	56195.164470	255	0.000368
56172.490040	23	0.000176	56183.827200	139	0.000215	56195.262210	256	0.000375
56172.588150	24	0.000560	56183.924730	140	0.000013	56195.360430	257	0.000857
56172.685740	25	0.000410	56184.022630	141	0.000179	56195.457810	258	0.000499
56172.783660	26	0.000599	56184.120290	142	0.000102	56195.554870	259	-0.000169
56172.881180	27	0.000383	56184.218090	143	0.000176	56195.653140	260	0.000363
56172.976400	28	-0.002126	56184.315620	144	-0.000029	56195.750570	261	0.000064
56173.076160	29	-0.000098	56184.413510	145	0.000121	56195.848480	262	0.000235
56173.173920	30	-0.000079	56184.509830	146	-0.001293	56195.945560	263	-0.000414
56173.271630	31	-0.000099	56184.608260	147	-0.000591	56196.043860	264	0.000151

Table 3—Continued

<i>BJD</i> (2400000+)	<i>E</i>	<i>O-C</i> (day)	<i>BJD</i> (2400000+)	<i>E</i>	<i>O-C</i> (day)	<i>BJD</i> (2400000+)	<i>E</i>	<i>O-C</i> (day)
56173.369600	32	0.000139	56184.706770	148	0.000187	56196.141820	265	0.000378
56173.467320	33	0.000118	56184.804520	149	0.000196	56196.239600	266	0.000422
56173.564820	34	-0.000112	56184.902510	150	0.000454	56196.336870	267	-0.000039
56173.661800	35	-0.000865	56185.000120	151	0.000333	56196.433770	268	-0.000877
56173.760780	36	0.000383	56185.097630	152	0.000104	56196.532390	269	0.000006
56173.858080	37	-0.000051	56185.195610	153	0.000357	56196.630590	270	0.000481
56173.956170	38	0.000303	56185.293170	154	0.000179	56196.727920	271	0.000076
56174.053490	39	-0.000106	56185.391270	155	0.000544	56196.825850	272	0.000266
56174.151310	40	-0.000021	56185.487430	156	-0.001027	56196.922920	273	-0.000392
56174.249310	41	0.000241	56185.585940	157	-0.000254	56197.021700	274	0.000647
56174.346610	42	-0.000194	56185.684580	158	0.000655	56197.119180	275	0.000396
56174.444900	43	0.000365	56185.781360	159	-0.000301	56197.216860	276	0.000343
56174.542940	44	0.000672	56185.879740	160	0.000350	56197.314680	277	0.000426
56174.640190	45	0.000185	56185.977530	161	0.000408	56197.412390	278	0.000402
56174.738300	46	0.000560	56186.074980	162	0.000120	56197.509550	279	-0.000165
56174.835800	47	0.000325	56186.172300	163	-0.000293	56197.608190	280	0.000743
56174.932460	48	-0.000742	56186.270320	164	-0.000007	56197.705680	281	0.000495
56175.031590	49	0.000653	56186.368060	165	-0.000004	56197.803480	282	0.000557
56175.128940	50	0.000271	56186.465960	166	0.000168	56197.900730	283	0.000075
56175.226190	51	-0.000219	56186.562190	167	-0.001343	56197.998930	284	0.000540
56175.324170	52	0.000030	56186.661870	168	0.000604	56198.096340	285	0.000220
56175.421840	53	-0.000037	56186.759170	169	0.000175	56198.193610	286	-0.000247
56175.519080	54	-0.000525	56186.857060	170	0.000324	56198.289770	287	-0.001821
56175.616900	55	-0.000444	56186.954730	171	0.000263	56198.389910	288	0.000590
56175.714790	56	-0.000288	56187.051170	172	-0.001029	56198.487710	289	0.000655
56175.812740	57	-0.000067	56187.148370	173	-0.001559	56198.582400	290	-0.002386
56175.910620	58	0.000078	56187.345610	175	0.000207	56198.682560	291	0.000041
56176.007950	59	-0.000328	56187.443480	176	0.000346	56198.780920	292	0.000660
56176.105370	60	-0.000640	56187.541470	177	0.000602	56198.878490	293	0.000495
56176.204030	61	0.000289	56187.638920	178	0.000319	56198.975990	294	0.000268
56176.299860	62	-0.001614	56187.735170	179	-0.001167	56199.073540	295	0.000086
56176.398510	63	-0.000701	56187.834130	180	0.000057	56199.269440	297	0.000517

Table 3—Continued

<i>BJD</i> (2400000+)	<i>E</i>	<i>O-C</i> (day)	<i>BJD</i> (2400000+)	<i>E</i>	<i>O-C</i> (day)	<i>BJD</i> (2400000+)	<i>E</i>	<i>O-C</i> (day)
56176.495590	64	-0.001359	56187.932060	181	0.000259	56199.366790	298	0.000131
56176.594100	65	-0.000576	56188.029460	182	-0.000078	56199.464140	299	-0.000256
56176.692390	66	-0.000020	56188.127800	183	0.000527	56199.562120	300	-0.000012
56176.790480	67	0.000332	56188.225240	184	0.000233	56199.660340	301	0.000478
56176.888620	68	0.000734	56188.322660	185	-0.000075	56199.756540	302	-0.001059
56176.984470	69	-0.001141	56188.418730	186	-0.001747	56199.855380	303	0.000055
56177.083640	70	0.000291	56188.518710	187	0.000505	56199.952760	304	-0.000306
56177.180220	71	-0.000860	56188.616330	188	0.000394	56200.051000	305	0.000202
56177.278600	72	-0.000221	56188.714240	189	0.000566	56200.147310	306	-0.001223
56177.376690	73	0.000135	56188.811590	190	0.000182	56200.246170	307	-0.000096
56177.472780	74	-0.001502	56188.908010	191	-0.001130	56200.343360	308	-0.000638
56177.571730	75	-0.000290	56189.006480	192	-0.000394	56200.442380	309	0.000648
56177.670260	76	0.000505	56189.103780	193	-0.000833	56200.539500	310	0.000037
56177.767040	77	-0.000447	56189.202680	194	0.000334	56200.637310	311	0.000108
56177.865110	78	-0.000108	56189.300300	195	0.000226	56200.733660	312	-0.001275
56177.962970	79	0.000021	56189.398040	196	0.000231	56200.833130	313	0.000466
56178.060870	80	0.000179	56189.495790	197	0.000244	56200.929980	314	-0.000420
56178.158400	81	-0.000026	56189.593620	198	0.000341	56201.028260	315	0.000124
56178.256420	82	0.000267	56189.691040	199	0.000031	56201.126550	316	0.000677
56178.354030	83	0.000139	56189.789080	200	0.000330	56201.223600	317	-0.000002
56178.451810	84	0.000185	56189.886530	201	0.000053	56201.321280	318	-0.000058
56178.549180	85	-0.000172	56189.984320	202	0.000104	56201.416990	319	-0.002085
56178.647280	86	0.000194	56190.082040	203	0.000096	56201.517390	320	0.000590
56178.745160	87	0.000335	56190.179890	204	0.000209	56201.614310	321	-0.000231
56178.842890	88	0.000328	56190.277520	205	0.000108	56201.712630	322	0.000362
56178.939190	89	-0.001099	56190.375500	206	0.000351	56201.810090	323	0.000081
56179.038220	90	0.000194	56190.472780	207	-0.000104	56201.907790	324	0.000049
56179.135860	91	0.000097	56190.570300	208	-0.000317	56202.005400	325	-0.000075
56179.233880	92	0.000387	56190.668720	209	0.000374	56202.103360	326	0.000149
56179.331530	93	0.000301	56190.766370	210	0.000291	56202.201190	327	0.000245
56179.428510	94	-0.000451	56190.864230	211	0.000408	56202.298940	328	0.000268
56179.527210	95	0.000520	56190.962000	212	0.000449	56202.396470	329	0.000060

Table 3—Continued

<i>BJD</i> (2400000+)	<i>E</i>	<i>O–C</i> (day)	<i>BJD</i> (2400000+)	<i>E</i>	<i>O–C</i> (day)	<i>BJD</i> (2400000+)	<i>E</i>	<i>O–C</i> (day)
56179.623860	96	−0.000570	56191.059450	213	0.000167	56202.493950	330	−0.000192
56179.722860	97	0.000702	56191.157180	214	0.000160	56202.591990	331	0.000110
56179.820160	98	0.000263	56191.254620	215	−0.000130	56202.689860	332	0.000252
56179.918350	99	0.000723	56191.352920	216	0.000429	56202.786320	333	−0.001022
56180.015740	100	0.000379	56191.450490	217	0.000272	56202.885650	334	0.000573
56180.113300	101	0.000206	56191.547920	218	−0.000030	56202.982810	335	−0.000003
56180.210870	102	0.000038	56191.645170	219	−0.000518	56203.078690	336	−0.001854
56180.306740	103	−0.001828	56191.743720	220	0.000298	56203.178700	337	0.000419
56180.406420	104	0.000120	56191.840570	221	−0.000588	56203.276280	338	0.000264
56180.504280	105	0.000248	56191.937960	222	−0.000929	56203.373270	339	−0.000481
56180.601890	106	0.000127	56192.036740	223	0.000114	56203.471890	340	0.000414
56180.699160	107	−0.000344	56192.134440	224	0.000079	56203.567240	341	−0.001976
56180.795700	108	−0.001533	56192.232960	225	0.000872	56203.667720	342	0.000768
56180.895050	109	0.000080	56192.329310	226	−0.000514	56203.764400	343	−0.000277
56180.992300	110	−0.000399	56192.427230	227	−0.000330	56203.862380	344	−0.000035
56181.089960	111	−0.000480	56192.525790	228	0.000494	56203.960520	345	0.000374
56181.188630	112	0.000464	56192.623420	229	0.000396	56204.058200	346	0.000315
56181.384160	114	0.000520	56192.719440	230	−0.001320	56204.155130	347	−0.000484
56181.481690	115	0.000322	56192.818760	231	0.000262	56204.253790	348	0.000439

Note. — T_{max} is the observed times light maxima of Q14.3. E: Cycle number. $O–C$ is in days. E and $O–C$ are based on the ephemeris formula: $T_{max}=T_0+P \times E=2456170.241912(0)+0.097734(1) \times E$.

Table 4. 351 times of Maximum Light and $O-C$ Values of Q15.3.

BJD (2400000+)	E	$O-C$ (day)	BJD (2400000+)	E	$O-C$ (day)	BJD (2400000+)	E	$O-C$ (day)
56269.247220	1013	-0.000625	56280.877690	1132	-0.000758	56292.605340	1252	-0.000334
56269.344600	1014	-0.000279	56280.974730	1133	-0.000064	56292.702980	1253	-0.000240
56269.442220	1015	-0.000161	56281.073020	1134	-0.000620	56292.800910	1254	-0.000436
56269.540260	1016	-0.000464	56281.170630	1135	-0.000496	56292.898380	1255	-0.000172
56269.637800	1017	-0.000275	56281.268270	1136	-0.000402	56292.996080	1256	-0.000138
56269.735600	1018	-0.000335	56281.365640	1137	-0.000038	56293.094110	1257	-0.000434
56269.833090	1019	-0.000091	56281.463680	1138	-0.000344	56293.191810	1258	-0.000400
56269.931190	1020	-0.000464	56281.561340	1139	-0.000271	56293.289020	1259	0.000124
56270.026710	1021	0.001753	56281.657010	1140	0.001793	56293.386910	1260	-0.000032
56270.126490	1022	-0.000293	56281.756560	1141	-0.000023	56293.484200	1261	0.000412
56270.223990	1023	-0.000059	56281.854750	1142	-0.000479	56293.582370	1262	-0.000024
56270.321960	1024	-0.000295	56281.952060	1143	-0.000055	56293.679450	1263	0.000630
56270.419330	1025	0.000069	56282.049780	1144	-0.000041	56293.778280	1264	-0.000466
56270.517320	1026	-0.000187	56282.148230	1145	-0.000757	56293.876100	1265	-0.000552
56270.615050	1027	-0.000183	56282.245210	1146	-0.000003	56293.973760	1266	-0.000479
56270.712930	1028	-0.000329	56282.343250	1147	-0.000309	56294.071190	1267	-0.000175
56270.809880	1029	0.000455	56282.441320	1148	-0.000645	56294.169130	1268	-0.000381
56270.908090	1030	-0.000021	56282.538800	1149	-0.000391	56294.267110	1269	-0.000627
56271.005880	1031	-0.000077	56282.636340	1150	-0.000197	56294.364320	1270	-0.000103
56271.103900	1032	-0.000363	56282.734100	1151	-0.000223	56294.462540	1271	-0.000589
56271.201530	1033	-0.000260	56282.831650	1152	-0.000039	56294.560070	1272	-0.000385
56271.299310	1034	-0.000306	56282.929800	1153	-0.000455	56294.657310	1273	0.000109
56271.396650	1035	0.000088	56283.026340	1154	0.000739	56294.755720	1274	-0.000567
56271.495050	1036	-0.000578	56283.125400	1155	-0.000587	56294.852860	1275	0.000027
56271.592500	1037	-0.000294	56283.221640	1156	0.000907	56294.950880	1276	-0.000259
56271.689900	1038	0.000040	56283.319670	1157	0.000611	56295.048320	1277	0.000035
56271.788110	1039	-0.000436	56283.418560	1158	-0.000545	56295.146050	1278	0.000039
56271.885550	1040	-0.000142	56283.613210	1160	0.000272	56295.244090	1279	-0.000267
56271.983470	1041	-0.000328	56283.711590	1161	-0.000374	56295.342260	1280	-0.000703
56272.081340	1042	-0.000464	56283.809150	1162	-0.000200	56295.439120	1281	0.000171
56272.178820	1043	-0.000210	56283.907030	1163	-0.000346	56295.537060	1282	-0.000035
56272.276530	1044	-0.000186	56284.004850	1164	-0.000432	56295.634240	1283	0.000519

Table 4—Continued

<i>BJD</i> (2400000+)	<i>E</i>	<i>O-C</i> (day)	<i>BJD</i> (2400000+)	<i>E</i>	<i>O-C</i> (day)	<i>BJD</i> (2400000+)	<i>E</i>	<i>O-C</i> (day)
56272.374310	1045	−0.000232	56284.102380	1165	−0.000228	56295.729570	1284	0.002923
56272.471890	1046	−0.000078	56284.199830	1166	0.000056	56295.829430	1285	0.000797
56272.569900	1047	−0.000354	56284.297950	1167	−0.000330	56295.926660	1286	0.001301
56272.667660	1048	−0.000380	56284.395300	1168	0.000054	56296.026600	1287	−0.000906
56272.765320	1049	−0.000306	56284.493620	1169	−0.000532	56296.123170	1288	0.000258
56272.863000	1050	−0.000252	56284.591050	1170	−0.000228	56296.221370	1289	−0.000208
56272.960750	1051	−0.000268	56284.687600	1171	0.000956	56296.317860	1290	0.001036
56273.058280	1052	−0.000064	56284.785250	1172	0.001040	56296.414040	1291	0.002590
56273.155470	1053	0.000480	56284.884340	1173	−0.000316	56296.511000	1292	0.003364
56273.253740	1054	−0.000057	56284.981990	1174	−0.000232	56296.611910	1293	0.000188
56273.351600	1055	−0.000183	56285.077820	1175	0.001672	56296.709150	1294	0.000682
56273.448980	1056	0.000171	56285.177470	1176	−0.000244	56296.807790	1295	−0.000224
56273.547220	1057	−0.000335	56285.275130	1177	−0.000170	56296.905310	1296	−0.000010
56273.644420	1058	0.000199	56285.372050	1178	0.000644	56297.002910	1297	0.000124
56273.741280	1059	0.001073	56285.467800	1179	0.002628	56297.100650	1298	0.000118
56273.938520	1061	−0.000699	56285.565450	1180	0.002712	56297.197940	1299	0.000562
56274.035230	1062	0.000325	56285.665800	1181	0.000095	56297.296390	1300	−0.000154
56274.133570	1063	−0.000281	56285.861330	1183	0.000033	56297.392410	1301	0.001560
56274.231150	1064	−0.000127	56285.959600	1184	−0.000503	56297.491260	1302	0.000444
56274.327110	1065	0.001647	56286.056500	1185	0.000331	56297.589490	1303	−0.000052
56274.426320	1066	0.000171	56286.155120	1186	−0.000555	56297.785160	1305	−0.000254
56274.524000	1067	0.000225	56286.252810	1187	−0.000511	56297.882660	1306	−0.000020
56274.622160	1068	−0.000201	56286.350580	1188	−0.000547	56297.980570	1307	−0.000196
56274.717460	1069	0.002233	56286.448300	1189	−0.000533	56298.078420	1308	−0.000313
56274.817810	1070	−0.000383	56286.545780	1190	−0.000279	56298.175800	1309	0.000041
56274.915010	1071	0.000151	56286.643040	1191	0.000195	56298.273730	1310	−0.000155
56275.013020	1072	−0.000125	56286.741250	1192	−0.000281	56298.372080	1311	−0.000771
56275.111010	1073	−0.000381	56286.838980	1193	−0.000277	56298.469360	1312	−0.000317
56275.208390	1074	−0.000027	56286.936360	1194	0.000077	56298.566870	1313	−0.000093
56275.306490	1075	−0.000394	56287.034590	1195	−0.000419	56298.665140	1314	−0.000629
56275.404250	1076	−0.000420	56287.131680	1196	0.000225	56298.761470	1315	0.000775
56275.501750	1077	−0.000186	56287.229660	1197	−0.000021	56298.860050	1316	−0.000071

Table 4—Continued

<i>BJD</i> (2400000+)	<i>E</i>	<i>O-C</i> (day)	<i>BJD</i> (2400000+)	<i>E</i>	<i>O-C</i> (day)	<i>BJD</i> (2400000+)	<i>E</i>	<i>O-C</i> (day)
56275.599390	1078	-0.000092	56287.327810	1198	-0.000437	56298.958050	1317	-0.000337
56275.697110	1079	-0.000078	56287.424240	1199	0.000867	56299.055550	1318	-0.000103
56275.794350	1080	0.000416	56287.522850	1200	-0.000009	56299.153290	1319	-0.000109
56275.892650	1081	-0.000150	56287.619450	1201	0.001125	56299.251170	1320	-0.000255
56275.990500	1082	-0.000266	56287.718830	1202	-0.000522	56299.348430	1321	0.000219
56276.087580	1083	0.000388	56287.816400	1203	-0.000358	56299.446700	1322	-0.000317
56276.185870	1084	-0.000168	56287.913600	1204	0.000176	56299.544730	1323	-0.000613
56276.283210	1085	0.000226	56288.011850	1205	-0.000340	56299.641680	1324	0.000171
56276.381720	1086	-0.000550	56288.109180	1206	0.000064	56299.739800	1325	-0.000215
56276.478890	1087	0.000014	56288.204520	1207	0.002458	56299.837890	1326	-0.000571
56276.576340	1088	0.000298	56288.305390	1208	-0.000678	56299.935590	1327	-0.000537
56276.674680	1089	-0.000308	56288.402210	1209	0.000236	56300.033080	1328	-0.000293
56276.772290	1090	-0.000184	56288.500550	1210	-0.000370	56300.130640	1329	-0.000119
56276.868770	1091	0.001070	56288.596770	1211	0.001144	56300.228430	1330	-0.000176
56276.967910	1092	-0.000336	56288.695490	1212	0.000158	56300.326330	1331	-0.000342
56277.065380	1093	-0.000072	56288.793390	1213	-0.000008	56300.424350	1332	-0.000628
56277.163150	1094	-0.000108	56288.891480	1214	-0.000364	56300.521650	1333	-0.000194
56277.261000	1095	-0.000224	56288.989070	1215	-0.000220	56300.617750	1334	0.001440
56277.358660	1096	-0.000151	56289.086150	1216	0.000434	56300.717080	1335	-0.000156
56277.456510	1097	-0.000267	56289.184800	1217	-0.000482	56300.814960	1336	-0.000302
56277.554080	1098	-0.000103	56289.282340	1218	-0.000288	56300.912480	1337	-0.000088
56277.652160	1099	-0.000449	56289.380040	1219	-0.000254	56301.010610	1338	-0.000484
56277.749520	1100	-0.000075	56289.477720	1220	-0.000200	56301.108370	1339	-0.000510
56277.945130	1102	-0.000217	56289.673180	1222	-0.000192	56301.303850	1341	-0.000522
56278.043150	1103	-0.000503	56289.771040	1223	-0.000318	56301.401420	1342	-0.000358
56278.140930	1104	-0.000549	56289.868640	1224	-0.000185	56301.498990	1343	-0.000194
56278.238740	1105	-0.000625	56289.965950	1225	0.000239	56301.597170	1344	-0.000640
56278.336400	1106	-0.000551	56290.064420	1226	-0.000497	56301.694170	1345	0.000094
56278.431730	1107	0.001853	56290.160130	1227	0.001527	56301.792080	1346	-0.000082
56278.531020	1108	0.000297	56290.259940	1228	-0.000549	56301.889740	1347	-0.000008
56278.629460	1109	-0.000409	56290.357620	1229	-0.000495	56301.987940	1348	-0.000474
56278.726700	1110	0.000085	56290.455440	1230	-0.000581	56302.085530	1349	-0.000330

Table 4—Continued

<i>BJD</i> (2400000+)	<i>E</i>	<i>O–C</i> (day)	<i>BJD</i> (2400000+)	<i>E</i>	<i>O–C</i> (day)	<i>BJD</i> (2400000+)	<i>E</i>	<i>O–C</i> (day)
56278.824790	1111	– 0.000271	56290.553010	1231	– 0.000417	56302.183430	1350	– 0.000496
56278.921720	1112	0.000533	56290.650280	1232	0.000047	56302.280910	1351	– 0.000243
56279.020440	1113	– 0.000453	56290.748250	1233	– 0.000189	56302.378520	1352	– 0.000119
56279.118050	1114	– 0.000329	56290.846020	1234	– 0.000225	56302.475930	1353	0.000205
56279.215760	1115	– 0.000305	56290.943910	1235	– 0.000381	56302.574170	1354	– 0.000301
56279.313150	1116	0.000039	56291.041540	1236	– 0.000277	56302.672260	1355	– 0.000657
56279.409370	1117	0.001553	56291.139230	1237	– 0.000233	56302.768850	1356	0.000487
56279.508740	1118	– 0.000084	56291.237000	1238	– 0.000269	56302.867500	1357	– 0.000429
56279.606250	1119	0.000140	56291.334790	1239	– 0.000325	56302.965130	1358	– 0.000325
56279.703700	1120	0.000424	56291.432170	1240	0.000029	56303.062770	1359	– 0.000231
56279.898990	1122	0.000602	56291.530090	1241	– 0.000157	56303.160200	1360	0.000073
56279.996930	1123	0.000396	56291.626750	1242	0.000917	56303.256340	1361	0.001667
56280.095200	1124	– 0.000140	56291.823050	1244	0.000085	56303.356080	1362	– 0.000339
56280.192880	1125	– 0.000086	56291.920980	1245	– 0.000112	56303.453260	1363	0.000215
56280.286690	1126	0.003838	56292.018040	1246	0.000562	56303.551610	1364	– 0.000401
56280.388840	1127	– 0.000578	56292.114970	1247	0.001366	56303.649390	1365	– 0.000447
56280.483200	1128	0.002796	56292.214200	1248	– 0.000130	56303.746520	1366	0.000157
56280.584210	1129	– 0.000480	56292.311990	1249	– 0.000186	56303.844710	1367	– 0.000299
56280.680730	1130	0.000734	56292.409870	1250	– 0.000332	56303.942220	1368	– 0.000075
56280.779730	1131	– 0.000532	56292.507010	1251	0.000262	56304.040060	1369	– 0.000181

Note. — T_{max} is the observed times light maxima of Q15.3. E: Cycle number. $O–C$ is in days. E and $O–C$ are based on the ephemeris formula: $T_{max}=T_0+P \times E=2456170.241912(0)+0.097734(1) \times E$.

Table 5. 322 times of Maximum Light and $O-C$ Values of Q16.3.

BJD (2400000+)	E	$O-C$ (day)	BJD (2400000+)	E	$O-C$ (day)	BJD (2400000+)	E	$O-C$ (day)
56359.162380	1933	-0.000284	56369.717590	2041	-0.000250	56380.465280	2151	0.002771
56359.259800	1934	0.000030	56369.814310	2042	0.000764	56380.564130	2152	0.001655
56359.358020	1935	-0.000457	56369.912870	2043	-0.000063	56380.664030	2153	-0.000511
56359.455730	1936	-0.000433	56370.010790	2044	-0.000249	56380.761410	2154	-0.000157
56359.553590	1937	-0.000559	56370.108430	2045	-0.000155	56380.858970	2155	0.000016
56359.650790	1938	-0.000025	56370.206570	2046	-0.000561	56380.956700	2156	0.000020
56359.748350	1939	0.000148	56370.303269	2047	0.000473	56381.055070	2157	-0.000616
56359.846140	1940	0.000092	56370.401730	2048	-0.000254	56381.151830	2158	0.000358
56359.943890	1941	0.000076	56370.499680	2049	-0.000470	56381.250210	2159	-0.000289
56360.042020	1942	-0.000320	56370.596596	2050	0.000348	56381.347850	2160	-0.000195
56360.139360	1943	0.000073	56370.694910	2051	-0.000233	56381.445770	2161	-0.000381
56360.236871	1944	0.000296	56370.792510	2052	-0.000099	56381.543410	2162	-0.000288
56360.334990	1945	-0.000089	56370.890860	2053	-0.000715	56381.641120	2163	-0.000264
56360.433060	1946	-0.000425	56370.988130	2054	-0.000251	56381.738450	2164	0.000140
56360.530830	1947	-0.000462	56371.085640	2055	-0.000028	56381.934710	2166	-0.000653
56360.627840	1948	0.000262	56371.183550	2056	-0.000204	56382.030950	2167	0.000841
56360.725940	1949	-0.000104	56371.280630	2057	0.000450	56382.129500	2168	0.000025
56360.823820	1950	-0.000250	56371.378620	2058	0.000193	56382.227340	2169	-0.000081
56360.921700	1951	-0.000397	56371.475570	2059	0.000977	56382.325380	2170	-0.000388
56361.019220	1952	-0.000183	56371.574460	2060	-0.000179	56382.420380	2171	0.002346
56361.116850	1953	-0.000079	56371.672420	2061	-0.000405	56382.520870	2172	-0.000410
56361.214470	1954	0.000034	56371.769780	2062	-0.000032	56382.617780	2173	0.000414
56361.312230	1955	0.000008	56371.867980	2063	-0.000498	56382.716120	2174	-0.000193
56361.410080	1956	-0.000108	56371.965300	2064	-0.000084	56382.814270	2175	-0.000609
56361.507840	1957	-0.000134	56372.062360	2065	0.000590	56382.911680	2176	-0.000285
56361.605440	1958	-0.000001	56372.159900	2066	0.000783	56383.009130	2177	-0.000001
56361.702870	1959	0.000303	56372.258650	2067	-0.000233	56383.105760	2178	0.001102
56361.800750	1960	0.000157	56372.355490	2068	0.000661	56383.204740	2179	-0.000144
56361.898570	1961	0.000071	56372.454240	2069	-0.000355	56383.301010	2180	0.001320
56361.996480	1962	-0.000106	56372.551120	2070	0.000498	56383.400210	2181	-0.000146
56362.094180	1963	-0.000072	56372.649430	2071	-0.000078	56383.497060	2182	0.000737
56362.191930	1964	-0.000088	56372.747700	2072	-0.000614	56383.595710	2183	-0.000179

Table 5—Continued

<i>BJD</i> (2400000+)	<i>E</i>	<i>O-C</i> (day)	<i>BJD</i> (2400000+)	<i>E</i>	<i>O-C</i> (day)	<i>BJD</i> (2400000+)	<i>E</i>	<i>O-C</i> (day)
56362.289900	1965	−0.000324	56372.844680	2073	0.000140	56383.693530	2184	−0.000265
56362.387470	1966	−0.000161	56372.942540	2074	0.000013	56383.791270	2185	−0.000271
56362.484990	1967	0.000053	56373.040660	2075	−0.000373	56383.889080	2186	−0.000348
56362.582540	1968	0.000237	56373.137930	2076	0.000091	56383.986200	2187	0.000266
56362.680990	1969	−0.000479	56373.236100	2077	−0.000345	56384.084340	2188	−0.000140
56362.778290	1970	−0.000046	56373.333630	2078	−0.000142	56384.182220	2189	−0.000287
56362.875180	1971	0.000798	56373.431490	2079	−0.000268	56384.280250	2190	−0.000583
56362.974260	1972	−0.000548	56373.528860	2080	0.000096	56384.377650	2191	−0.000249
56363.070610	1973	0.000836	56373.626509	2081	0.000181	56384.475830	2192	−0.000695
56363.169520	1974	−0.000341	56373.724830	2082	−0.000407	56384.573190	2193	−0.000322
56363.267200	1975	−0.000287	56373.822560	2083	−0.000403	56384.671350	2194	−0.000748
56363.365161	1976	−0.000514	56373.920060	2084	−0.000169	56384.866320	2196	−0.000250
56363.462480	1977	−0.000099	56374.018050	2085	−0.000426	56384.963520	2197	0.000283
56363.560410	1978	−0.000296	56374.115360	2086	−0.000002	56385.061650	2198	−0.000113
56363.658330	1979	−0.000482	56374.213540	2087	−0.000448	56385.156790	2199	0.002481
56363.755120	1980	0.000462	56374.310950	2088	−0.000124	56385.257060	2200	−0.000055
56363.853410	1981	−0.000095	56374.408330	2089	0.000229	56385.355300	2201	−0.000562
56363.951160	1982	−0.000111	56374.506440	2090	−0.000147	56385.451510	2202	0.000962
56364.048870	1983	−0.000087	56374.604460	2091	−0.000433	56385.549890	2203	0.000316
56364.146780	1984	−0.000263	56374.701770	2092	−0.000009	56385.648100	2204	−0.000160
56364.244430	1985	−0.000180	56374.798750	2093	0.000744	56385.745810	2205	−0.000137
56364.342300	1986	−0.000316	56374.897370	2094	−0.000142	56385.843980	2206	−0.000573
56364.440060	1987	−0.000342	56374.995260	2095	−0.000298	56385.941550	2207	−0.000409
56364.537380	1988	0.000072	56375.093070	2096	−0.000374	56386.039360	2208	−0.000485
56364.634870	1989	0.000315	56375.190460	2097	−0.000031	56386.136510	2209	0.000098
56364.732730	1990	0.000189	56375.288140	2098	0.000023	56386.234200	2210	0.000142
56364.830670	1991	−0.000017	56375.386270	2099	−0.000373	56386.331910	2211	0.000166
56364.927800	1992	0.000587	56375.483470	2100	0.000161	56386.430430	2212	−0.000620
56365.025040	1993	0.001080	56375.581020	2101	0.000344	56386.527780	2213	−0.000237
56365.123450	1994	0.000404	56375.679620	2102	−0.000522	56386.625160	2214	0.000117
56365.221480	1995	0.000108	56375.777300	2103	−0.000468	56386.723150	2215	−0.000139
56365.319290	1996	0.000032	56375.874800	2104	−0.000234	56386.820590	2216	0.000154

Table 5—Continued

<i>BJD</i> (2400000+)	<i>E</i>	<i>O-C</i> (day)	<i>BJD</i> (2400000+)	<i>E</i>	<i>O-C</i> (day)	<i>BJD</i> (2400000+)	<i>E</i>	<i>O-C</i> (day)
56365.417230	1997	−0.000175	56375.972440	2105	−0.000141	56386.918480	2217	−0.000002
56365.515290	1998	−0.000501	56376.069990	2106	0.000043	56387.015980	2218	0.000232
56365.612840	1999	−0.000317	56376.167090	2107	0.000677	56387.113720	2219	0.000226
56365.710560	2000	−0.000303	56376.265470	2108	0.000031	56387.211480	2220	0.000199
56365.808050	2001	−0.000060	56376.363830	2109	−0.000596	56387.309030	2221	0.000383
56365.905270	2002	0.000454	56376.461400	2110	−0.000432	56387.407510	2222	−0.000363
56366.003400	2003	0.000058	56376.558470	2111	0.000232	56387.504570	2223	0.000311
56366.101190	2004	0.000002	56376.656860	2112	−0.000425	56387.602880	2224	−0.000266
56366.198400	2005	0.000525	56376.754540	2113	−0.000371	56387.700910	2225	−0.000562
56366.296590	2006	0.000069	56376.852270	2114	−0.000367	56387.798680	2226	−0.000598
56366.394330	2007	0.000063	56376.950080	2115	−0.000443	56387.896150	2227	−0.000334
56366.492380	2008	−0.000254	56377.047480	2116	−0.000110	56387.993850	2228	−0.000301
56366.590170	2009	−0.000310	56377.145270	2117	−0.000166	56388.091580	2229	−0.000297
56366.687580	2010	0.000014	56377.243080	2118	−0.000242	56388.188280	2230	0.000737
56366.785600	2011	−0.000272	56377.340500	2119	0.000072	56388.286520	2231	0.000231
56366.883450	2012	−0.000389	56377.438570	2120	−0.000265	56388.384710	2232	−0.000226
56366.981040	2013	−0.000245	56377.536090	2121	−0.000051	56388.481870	2233	0.000348
56367.077570	2014	0.000959	56377.633540	2122	0.000233	56388.580020	2234	−0.000068
56367.176360	2015	−0.000097	56377.731640	2123	−0.000133	56388.677950	2235	−0.000264
56367.274280	2016	−0.000284	56377.829480	2124	−0.000240	56388.775870	2236	−0.000451
56367.371830	2017	−0.000100	56377.927480	2125	−0.000506	56388.873480	2237	−0.000327
56367.469090	2018	0.000374	56378.024940	2126	−0.000232	56388.971130	2238	−0.000243
56367.567430	2019	−0.000232	56378.122640	2127	−0.000198	56389.067460	2239	0.001160
56367.665390	2020	−0.000459	56378.220520	2128	−0.000345	56389.166750	2240	−0.000396
56367.762730	2021	−0.000065	56378.317870	2129	0.000039	56389.264590	2241	−0.000502
56367.860860	2022	−0.000461	56378.415330	2130	0.000313	56389.361840	2242	−0.000018
56367.957990	2023	0.000143	56378.513730	2131	−0.000353	56389.459630	2243	−0.000075
56368.055900	2024	−0.000034	56378.611170	2132	−0.000060	56389.557060	2244	0.000229
56368.153380	2025	0.000220	56378.707970	2133	0.000874	56389.655270	2245	−0.000247
56368.251290	2026	0.000044	56378.807000	2134	−0.000422	56389.753070	2246	−0.000313
56368.349190	2027	−0.000122	56378.904520	2135	−0.000209	56389.850360	2247	0.000130
56368.447010	2028	−0.000209	56379.002160	2136	−0.000115	56389.948170	2248	0.000054

Table 5—Continued

<i>BJD</i> (2400000+)	<i>E</i>	<i>O–C</i> (day)	<i>BJD</i> (2400000+)	<i>E</i>	<i>O–C</i> (day)	<i>BJD</i> (2400000+)	<i>E</i>	<i>O–C</i> (day)
56368.544720	2029	– 0.000185	56379.100310	2137	– 0.000531	56390.044220	2249	0.001738
56368.632050	2030	0.010219	56379.197330	2138	0.000183	56390.144030	2250	– 0.000338
56368.740520	2031	– 0.000517	56379.295410	2139	– 0.000164	56390.241880	2251	– 0.000455
56368.838140	2032	– 0.000404	56379.393430	2140	– 0.000450	56390.338900	2252	0.000259
56368.936030	2033	– 0.000560	56379.588270	2142	0.000178	56390.437340	2253	– 0.000447
56369.033720	2034	– 0.000516	56379.685640	2143	0.000541	56390.534920	2254	– 0.000293
56369.131020	2035	– 0.000083	56379.784000	2144	– 0.000085	56390.632650	2255	– 0.000290
56369.228570	2036	0.000101	56379.880580	2145	0.001069	56390.730080	2256	0.000014
56369.326500	2037	– 0.000095	56379.979280	2146	0.000103	56390.828220	2257	– 0.000392
56369.423980	2038	0.000159	56380.075360	2147	0.001756	56390.925920	2258	– 0.000358
56369.522210	2039	– 0.000338	56380.174850	2148	0.000000			
56369.618390	2040	0.001216	56380.369930	2150	0.000388			

Note. — T_{max} is the observed times light maxima of Q16.3. E: Cycle number. $O–C$ is in days. E and $O–C$ are based on the ephemeris formula: $T_{max}=T_0+P \times E=2456170.241912(0)+0.097734(1) \times E$.